International Journal of Scientific Research in Computer Science, Engineering and Information Technology
© 2017 IJSRCSEIT | Volume 2 | Issue5 | ISSN : 2456-3307

A Fast Method for Haze Evacuation in Satellite Images by Using Bilateral Filter

[1]M.Vasudeva Reddy, [2]Dr.T.Ramashri

[1]Research Scholar, Rayalaseema University, Kurnool, India

[2]Professor, S.V.University, Tirupati, Andhra Pradesh, India

ABSTRACT

The perceivability of the open air images is degraded on account of terrible climate conditions. Robust solutions to this issue, a simple and novel strategy to take out the haze from satellite remote sensing images using Bilateral filter. The task is challenging due to variations in dark channel prior, air light, transmission map and radiance map. The nearness of haze in the atmosphere degrades the quality of images captured by visible camera sensors. The expulsion of haze is commonly performed under the statistical strategies. Due to haziness, an image generally lost shading and edges. So de hazing strategy restores edge losses and shading impacts seriously. The strategy plays out a per-pixel operation, which is direct to create develop and then apply the bilateral filter to improve the image quality. We compare our methodology with state-of-art criteria like Gaussian filter. Exploratory outcomes show that the proposed strategy can permit a quick execution, it is viable for visual engaging and shading loyalty contrasted with some state-of-the-art methods.

Keywords : Gaussian filter, Bilateral filter, PSNR, MSE and Normalized Cross Correlation.

I. INTRODUCTION

Haze is an irritating variable when it appears in the image since it causes poor perceivability. This is the real issue utilized as a part of different fields including agriculture, forestry, metrology, and military. Be that as it may, boundless utilization of satellite remote sensing images is predicated on superb images.

Poor perceivability because of haze is caused by suspended particles in the atomsphere . The approaching light from a scene or thing is scaterred because of this and henceforth it is constrict till it achieves the camera.This debasement will make the image lose complexity and shading rightness. Moreover, the airlight which influence the image relies upon the profundity of the scene.This information is generally utilized for dehazing issues. We likewise receive this intimation to tackle the haze evacuation issue. Imagehaze evacuation has gotten a developing interest as of late. An ever increasing number of strategies are presented in the previous three years.By the by, dehazing is a testing theme since the haze is subject to the obscure depth data. Frequently, the images of open air scenes are debased by awful climate conditions.In such cases, environmental marvels like haze corrupt altogether the perceivability of the caught scene. Since the airborne is moistened by extra particles, the reflected light is scattered and accordingly, inaccessible objects and parts of the scene are less obvious, which is portrayed by decreased differentiation and blurred colors.Dark channel [2][9] in the neighboring pixels window to appraise the airlight and transmission outline by delicate tangling to refine the image. The strategy fundamentally improves the nature of hazyimages [1]. Additionally, the strategy creating transmission map can't ensure edge preseving and subsequently sharpness of the image corrupts.

Dehazing is very required in consumer photography and PC vision applications. Since numerous PC vision applications are experience the ill effects of low-differentiate scene radiance. For instance, there is an issue of haze in submerged images. There are numerous techniques accessible to expel haze from open air image.

II. EXISTING METHOD

2. Bilateral Filter

We utilize a low-pass bilateral filter to refine the radiance map [14]. Bilateral filter is a nonlinear filter that smooth's the images. We smooth the radiance map using a low-pass bilateral channel, the refined radiance outline V(x) can be expressed as

$$V(x) = \frac{\mathbf{1}}{\boldsymbol{W^g}} \sum_{\boldsymbol{y \epsilon S}} \boldsymbol{G_\sigma}(||\boldsymbol{x}-\boldsymbol{y}||)\bar{\boldsymbol{V}}(y) \qquad (1)$$

Where $\boldsymbol{W^g}$ is the entirety weight of the neighbourhood patch centered at pixel x, x is a original image and y is a filter image

$$\boldsymbol{W^g} = \boldsymbol{G_\sigma}\ (||\boldsymbol{x}-\boldsymbol{y}||) \qquad (2)$$

Here G is a Bilateral function, and the parameter a represents the size of the area used to smooth a pixel. Standard deviation of the Bilateral dissemination, determined as a scalar or 3- component vector of positive values. As per the low-pass Bilateral filter, those pixels close to the focused pixel x will get substantial weight. With the refined radiance map.

The basic idea underlying bilateral filtering is to do in the range of an image what traditional filters do in its domain. Two pixels can be *close* to one another, that is, occupy nearby spatial location, or they can be *similar* to one another, that is, have nearby values, possibly in a perceptually meaningful fashion.

Combined domain and range filtering will be denoted as bilateral filtering. It replaces the pixel value at **x** with an average of similar and nearby pixel values. In smooth regions, pixel values in a small neighbourhood are similar to each other, and the bilateral filter acts essentially as a standard domain filter, averaging away the small, weakly correlated differences between pixel values caused by noise. Consider now a sharp boundary between a dark and a bright region, as in figure 1(a).

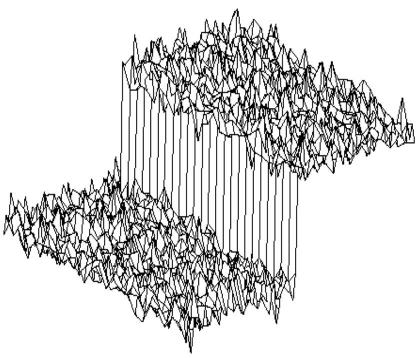

(a)

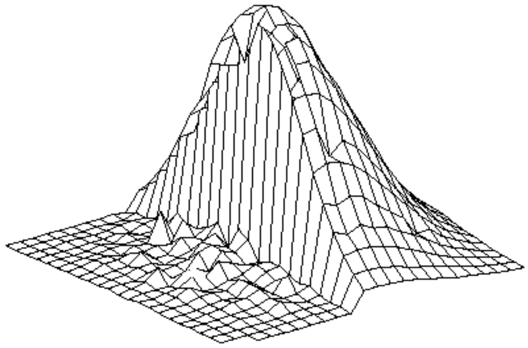

(b)

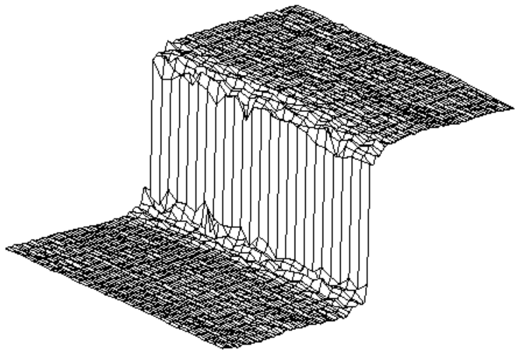

(c)

Figure 1: figure representing bilateral filter performance on image

When the bilateral filter is centred, say, on a pixel on the bright side of the boundary, the similarity function *s* assumes values close to one for pixels on the same side, and values close to zero for pixels on the dark side. The similarity function is shown in figure 1(b) for a 23x23 filter support centred two pixels to the right of the step in figure 1(a). The normalization term *k(**x**)* ensures that the weights for all the pixels add up to one. As a result, the filter replaces the bright pixel at the centre by an average of the bright pixels in its vicinity, and essentially ignores the dark pixels. Conversely, when the filter is entered on a dark pixel, the bright pixels are ignored instead. Thus, as shown in figure 1(c), good filtering behaviour is achieved at the boundaries, thanks to the domain component of the filter, and crisp edges are preserved at the same time, thanks to the range component.

A much better result can be obtained with bilateral filtering. In fact, a bilateral filter allows combining the three colour bands appropriately, and measuring photometric distances between pixels in the combined space. Moreover, this combined distance can be made to correspond closely to perceived dissimilarity by using Euclidean distance in the CIE-Lab colour space. This colour space is based on a large body of psychophysical data concerning colour-matching experiments performed by human observers. In this space, small Euclidean distances are designed to correlate strongly with the perception of colour discrepancy as experienced by an average colour-normal human observer. Thus, in a sense, bilateral filtering performed in the CIE-Lab colour space is the most natural type of filtering for colour images: only perceptually similar colors are averaged together, and only perceptually important edges are preserved.

III. PROPOSED METHOD

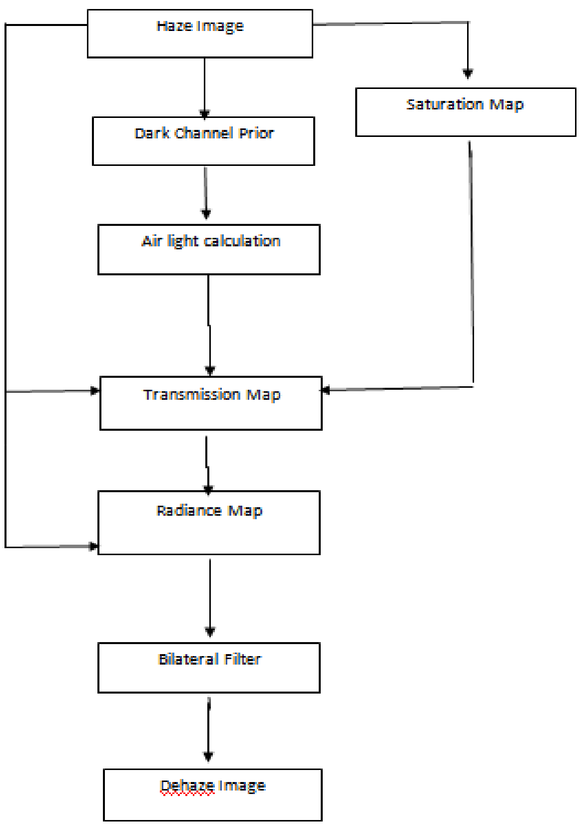

Figiure2. Block diagram of Proposed Method

This model utilized for the arrangement of image within the sight of awful environmental conditions. Image quality is debased because of the nearness of generous particles in the climate, which have noteworthy size between 1-10 µm.

The light originating from a camera is ingested and scattered by these air particles. Accept that this haze demonstrate is direct model. From the meaning of linearity in this model [6] just pixel position is changed. This intangibility is happened by two basic: Direct attenuation and Air light. Furthermore, it is depict as follow:

$$I(x) = J(x)*t(x) + A*(1-t(x) \qquad (3)$$

Where I (x) is the observed intensity of the x^{th} pixel, J (x) is the scene radiance the genuine nature that we need to recoup), A is the atmospheric light, and t is the transmission medium describing the portion of the light that is not scattered and reaches direct to the camera.
In the condition initially term, J(x)*t(x) is known as the direct attenuation; the second term, A*(1-t(x)) is called air light. This haze display is straight forwardly reached out to each RGB part of a shading image.

Dark Channel Prior

Dark channel prior [9] to the haze free open air images, which underpins that a large portion of nearby areas barring the sky have low force in no less than one shading channel. The forces of these dark pixels are principally caused by Shadows, Colourful protests or surfaces and Dark objects or surfaces [2]. Correspondingly, it has been observed that the pixels in hazy areas have high esteems in every single shading channel. The dark channel is characterized as where is a channel of and is a nearby neighbourhood focused at. In view of the dark channel earlier, is a steady in a neighbourhood image patch. In this manner, we characterize the nearby transmission as and bring the min operation with a neighbourhood patch on.

It is coarsely great yet contains some block impacts, since the climatic light isn't generally steady in a patch. In other words, a neighbourhood patch may contain the locale where the scene depth is intermittent. For maintaining a strategic distance from this issue, evaluated the environmental light utilizing bilateral filter on the negligible part of the hazy image.
It in light of the perception that no less than one shading channel has a few pixels whose intensity values are low and near zero. In this it is processed as

$$J^d=\min_{y\epsilon\Omega(x)}((1-\sigma_{rgb})*\mu_{c\epsilon\{r,g,b\}}(J^c(y)) \qquad (4)$$

Where J^ca color channel of J, µ is is a mean and σ_{rgb} is a standard deviation of r, g, b intensity values and Ω(x) is a nearby patch focused at x.

We consider top 1% pixels in registering airlight and discover the pixel which has most extreme estimation of J^d in its dull channel among the pixels in light of equation(4). The estimation of I at that pixel is considered as airlight.

Estimation of atmospheric light

By and large, the atmospheric light[7] is constantly considered as the brightest intensity in the whole image on the grounds that a lot of haze makes the object scene brighter than itself. The fundamental thought of this technique is that atmospheric light ought to be assessed from the locale with brighter intensity [6] and less surface.

The atmospheric light is assessed as the value that has minimal separation to the unadulterated white. Pad Array comprises of zeros. It depends on Pad size, is a vector of nonnegative numbers that indicates both the amount of padding to add and the measurement along which to include it. The estimation of a component in the vector determines the amount of padding to add. The request of the component in the vector indicates the dimension along which to include the padding.

In this work, we choose this technique since it is basic however productive. Nonetheless, it isn't vigorous on the grounds that the evaluated climatic light might be the noise[13]. So we respect the mean estimation of the best 5% brightest values in the chose area as the air light to reject the noise impact viably.

Saturation Map

It changes over the Haze image to the equal HSV image [10]. RGB is a 3-image exhibit whose three planes contain the red, green and blue segments for the image. HSV is returned as a 3-picture exhibit whose three planes contain the Hue, Saturation and value parts of the image.

Transmission Map and Radiance Map

It is observed that the saturation of shading in a hazy image diminishes with the thickness of haze, which thus relies upon depth, or separation of the object. In this strategy, we consolidate saturation map and airlight to get a more exact transmission map clearer image [5]. The transmission outline is figured by utilizing

$$t=1-f(S)(\boldsymbol{min_{y\epsilon\Omega(x)}})((1-\boldsymbol{\sigma_{rgb}})*\boldsymbol{\mu_{c\epsilon\{r,g,b\}}}(\frac{\boldsymbol{I^c(y)}}{\boldsymbol{A^c}}))) \quad (5)$$

Where f(s) reliesuponthe saturation of the input image at x. It is expressed as

$$f(S)=0.8-(0.2*S) \quad (6)$$

where S is saturation of the pixel ($0 \leq S \leq 1$). We outline estimation of the pixels to f(S) to improve the output as we observed lesser saturation in an object that are far away and have more haze. If the saturation is less, f(S) will be progressively and the other way around. This evacuates conflicting shading patches in the yield [13].

We estimate scene radiance as

$$J(x)=\frac{\boldsymbol{I(x)-A}}{\boldsymbol{max(t(x),t_o)}}+A \quad (7)$$

Where $\boldsymbol{t_o}$ is a factor to confine the noise level.

A bilateral filter is a non-linear, edge-preserving, and smoothing filter for images. It replaces the intensity of each pixel with a weighted average of intensity values from nearby pixels [8]. This weight can be based on a bilateral distribution. Crucially, the weights depend not only on Euclidean distance of pixels, but also on the radiometric difference. It is observed that the transmission delineate haze exclusion approach creates blocks and artifacts along the edges. Yet, soft matting by processing 3 transmission maps using 3 different block sizes (3*3,5*5,7*7) and generate radiance map for all block sizes followed by cross bilateral filtering. The transmission maps and comparing radiance images.

For a greater square size, the impact is considerably more however, it reduces noise. It can generate more artifact in the image for block size 7*7 generate more artifacts in the image along the edges as compared to 3*3. Whereas the noise level in 7*7 is less as compared to 3*3.

This approach of ours reduces noise and eliminate the need for soft matting thus improving the instance required for processing. Bilateral filter does weighted averaging of pixels across multiple frames (radiance image) obtained. The radiance map corresponding to 3*3 block is considered as a position as it conserves most of the edge or gradient information in the image. The filtering is performed on intensity(Y) of the radiance image.

$$Y_{ij}=\frac{1}{K}\sum_{K=1}^{N}\left\{e^{\left(\frac{-\left(Y_{ij(3*3)}-Y_{ij(k_1*k_1)}\right)^2}{2\sigma_m^2}\right)}Y_{ij(k1*k1)}\right\} \quad (8)$$

Where Y_{ij} is the filtered output at (i,j) pixel location, N is the number of frames, k1 indicates block size, σ_m is a constant and K is normalizing factor given by

$$K=\sum_{K=1}^{N}\left\{e^{\left(\frac{-\left(Y_{ij(3*3)}-Y_{ij(k_1*k_1)}\right)^2}{2\sigma_m^2}\right)}\right\} \quad (9)$$

The value of σ_m depends on the uniqueness of noise. The weights depend on difference of pixel of current frame from pixel of reference frame. If the deviation is less the weights tend to become equal, otherwise haze in the Image reduces the contrast of captured image. Hence, contrast enhancement is performing to restore the contrast. Since the noise component is reduced in the previous step the contrast may be enhanced without enhancing the noise.

$$I(x,y) = \frac{1}{1-m^{\gamma}+\left({}^{m}/_{r(x,y)}\right)^{\gamma}} \qquad (10)$$

Where m is a threshold, r(x,y) is input intensity and γ is contrast enhancement factor to produce output I(x,y). Based on empirical observation using a number of images we assumed m to be 0.8 times the mean intensity of the image and γ =2.0 in the present work

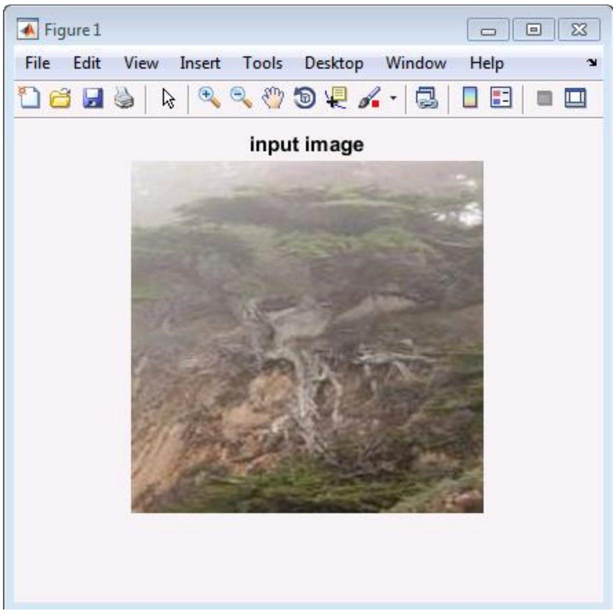

Figure 3. Haze Image

Figure 3 demonstrates Image is effected by a loss of contrast in the subject, because of the impact of light scattering through the haze particles

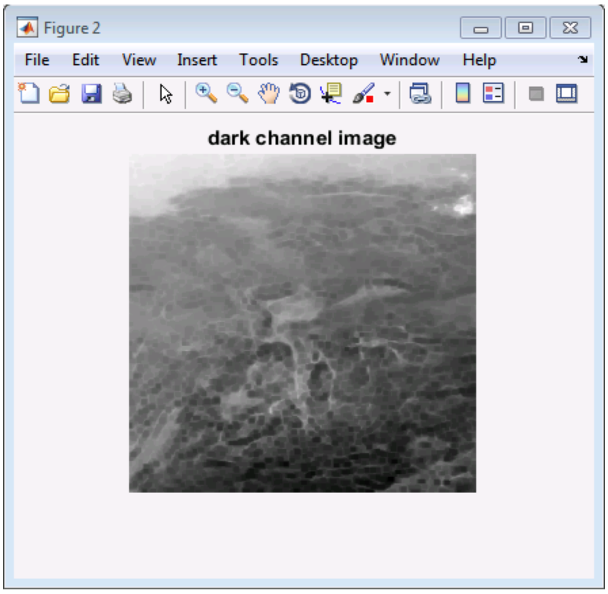

Figure4. Dark Channel Prior Image

Figure 4demonstrates the dull channels from hazy images as the base an incentive for every one of the channels and every one of the pixels in that patch and create pixels that have values far over zero.

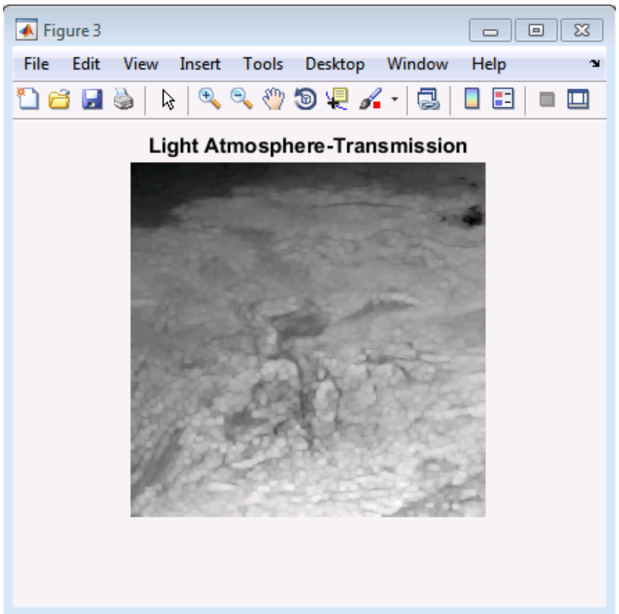

Figure 5. Airlight Image

Figure 5shows to get the atmospheric light, the normal of the pixels in the haze image that compare to the best lightest 0.01% in the dark channel. In this manner, it has 3 components, the average values for each shading channel.

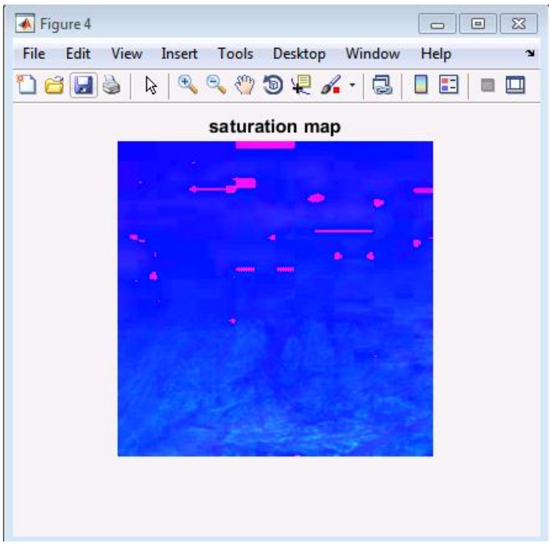

Figure6. Saturation Map

Figure 6 demonstrates changing over haze image into Hue saturation value..The columns of the input matrix represent intensities of red, green, and blue, individually. The columns of the output matrix represent hue, saturation, and value, respectively.

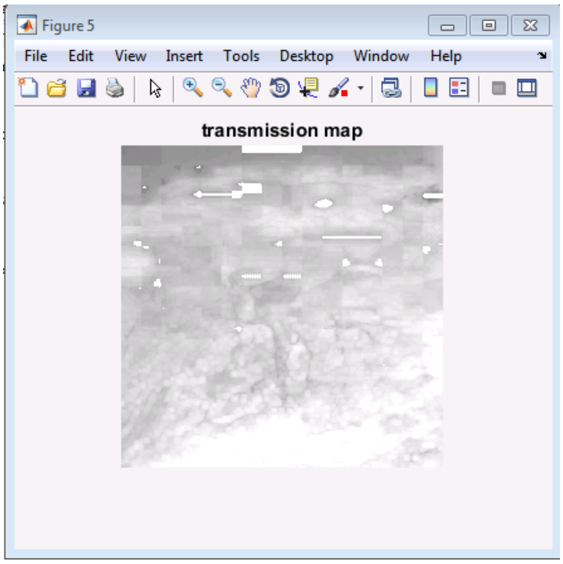

Figure 7 demonstrates it includes every component in exhibit airlight with the relating components in cluster saturation map and returns of the total in the comparing component the output exhibit as transmission map.

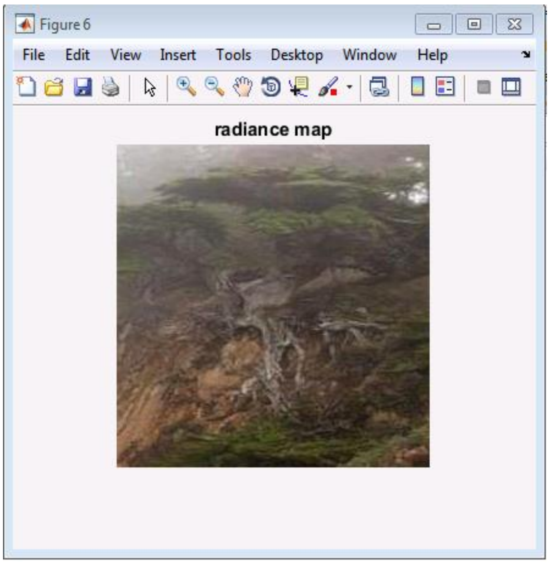

Figure7. Radiance Map

Figure 8 indicates expands the intensity of an image by considering the maximum pixels of airlight, saturation map and transmission map.

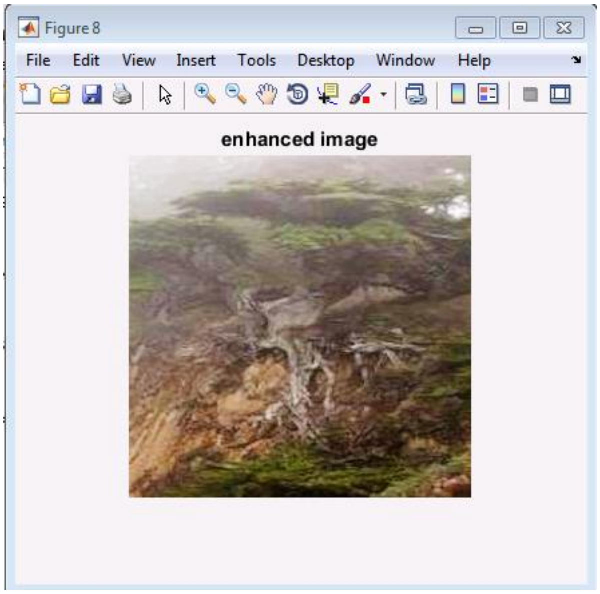

Figure8. Dehaze Image

Figure 9 demonstrates every individual pixel is supplanted with a Bilateral shaped with the same aggregate weight from the first intensity value. It renders little structures undetectable and smoothens sharp edges.

IV. RESULTS AND DISCUSSION

Utilizing a recently exhibited image prior-dark channel prior, haze removal for a statellite remote sensing image additional information is formulated as a specific filtering issue and an enhanced filtering scheme is based Bilateral filter. In the presented algorithm, the airlight, transmission map and radiance map can be evaluatedand extracted easily. At that point utilizing a bilateral filter, the trasmission map further refined. Results demonstrate the exhibited strategy abilities to remove the haze layer and achieve real-time performance layer and achieve real time performance.

Table 1. Comparison Table

Parameters	Existing (Gaussian Filter)	Proposed (Bilateral Filter)
Peak Signal-Noise Ratio	53.7878	55.2724
Mean Square Error	0.2718	0.1931
Normalized cross correlation	0.0035	0.8545

From the Table 1, on satellite remote sensing images of different datasets demonstrates that our novel strategy is viable for dehazing. Hence in the overall implementation peak signal-noise-ratio, mean square error and normalized cross correlation is better than Gaussian filter.

VII. CONCLUSION

For some PC vision applications, haze removal algorithm turned out to be more helpful. It was found that most of the existing strategies gradient reversal issue that is no method is exact for various sort of conditions. The issue of over- brightening is an issue for haze from the satellite remote sensing images. We concentrate on an enhanced atmospheric scattering model by considering noise and haze simultaneously. Gaussian filter is used as state-of-art criteria for haze removal in imagery, which reduces haze and some image information is lost which can overcome in our methodology. The probability of back likelihood in light of bilateral filter is assessed by the factual earlier and target supposition of debased image. Meanwhile, we concentrate more on the effectiveness by choosing the transmission map to get the scene radiance. Bilateral filter which can help to achieve the balance between dehazing and denoising. The experimental results demonstrate that our approach is effective, particularly in challenging scenes with both haze and noise. However, colour distortion still exists which will be involved in our future work.

V. ACKNOWLEDGEMENTS

This paper is dedicated to our Parents, Colleagues and Friends for their help without which the effective fruition of this paper isn't conceivable.

VI. REFERENCES

[1] R. Fattal, "**Single image dehazing**," ACM Transactions on Graphics, vol. 27, no. 3, article 72, pp. 1–9, 2008.

[2] T. M. Bui, H. N. Tran, W. Kim, and S. Kim, "**Segmenting dark channel prior in single image dehazing**," Electronics Letters, vol. 50, no. 7, pp. 516–518, 2014.

[3] C. O. Ancuti and C. Ancuti, "**Single image dehazing by multi-scale fusion**," IEEE Transactions on Image Processing, vol. 22, no. 8, pp. 3271–3282, 2013

[4] W. Wang, W. Li, Q. Guan, and M. Qi, "**Multi scale single image dehazing based on adaptive wavelet fusion**," Mathematical Problems in Engineering, vol. 2015, Article ID 131082, 14 pages, 2015.

[5] S.-C. Huang, J.-H. Ye, and B.-H. Chen, "**An advanced single-image visibility restoration algorithm for real-world hazy scenes**," IEEE Transactions on Industrial Electronics, vol. 62, no. 5, pp. 2962–2972, 2015.

[6] G. Meng, Y. Wang, J. Duan, S. Xiang, and C. Pan, "**Efficient image dehazing with boundary constraint and contextual regularization**," in Proceedings of the 14th IEEE International Conference on Computer Vision (ICCV '13), pp. 617–624, IEEE, Sydney, Australia, December 2013.

[7] S.-C. Huang, B.-H. Chen, and W.-J. Wang, "**Visibility restoration of single hazy images captured in real-world weather conditions,**" IEEE Transactions on Circuits and Systems for Video Technology, vol. 24, no. 10, pp. 1814–1824, 2014.

[8] Q. Zhu, J. Mai, and L. Shao, "**A fast single image haze removal algorithm using color attenuation prior**," IEEE Transactions on Image Processing, vol. 24, no. 11, pp. 3522–3533, 2015
[9] D.-Y. Zhang, M.-Y. Ju, and X.-M. Wang, "**A fast image haze removal algorithm using dark channel prior,**" Acta Electronica Sinica, vol. 43, no. 7, pp. 1437–1443, 2015.
[10] Q. Zhu, J. Mai, and L. Shao, "**A fast single image haze removal algorithm using color attenuation prior**," IEEE Transactions on Image Processing, vol. 24, no. 11, pp. 3522–3533, 2015.
[11] C. T. Thurow, **Real-Time Image Dehazing, Technical University**, Berlin, Germany, 2011.
[12] W. Ren, S. Liu, H. Zhang, J. Pan, X. Cao, and M.-H. Yang, "**Single image dehazing via multi-scale convolutional neural networks**," in ECCV. Springer, 2016, pp. 154–169.
[13] B. Cai, X. Xu, K. Jia, C. Qing, and D. Tao, "**Dehazenet: An end-to-end system for single image haze removal**," IEEE TIP, vol. 25, no. 11, pp. 5187–5198, 2016.
[14] K. Tang, J. Yang, and J. Wang, "**Investigating haze-relevant features in a learning framework for image dehazing**," in CVPR, 2014, pp. 2995– 3000